Available online at www.sciencedirect.com
SCIENCE DIRECT®
Vision Research 44 (2004) 2989–3000
Vision Research
www.elsevier.com/locate/visres

Effect of stimulus localisation on motion-onset VEP

J. Kremláček *, M. Kuba, J. Chlubnová, Z. Kubová

Department of Pathophysiology, Faculty of Medicine, Charles University, Simkova 870, 500 01 Hradec Králové, Czech Republic

Received 19 January 2004; received in revised form 20 May 2004

Abstract

Reliable motion-onset visual evoked potentials (result of the dorsal stream activation) were recorded to motion stimuli with the temporal frequency of five cycles per seconds in 20 different locations with eccentricity up to 42° to periphery of the visual field. Amplitudes and latencies of the positive–negative–positive (P1–N1–P2; 84–144–208 ms) complex were evaluated in occipital (O_Z and two derivations 5 cm to the left and right from O_Z) and central region (C_Z) in 10 subjects.

We observed: (1) Shortening of the N1 latency toward periphery of the visual field. (2) The N1 amplitude maximum and latency minimum moved from occipital into central region (C_Z derivation) as stimulus moved from centre toward periphery of visual field. (3) The P1 and N1 peaks displayed significantly greater amplitudes and shorter latencies when the lower part of the visual field was stimulated. (4) The N1 peak changed lateralisation of its maximum amplitude in dependence on the eccentricity. Up to 17°, it corresponds to striate projection of the ''optic radiation'' whilst more in periphery, there was paradoxical lateralisation of higher amplitude and shorter latency. The retinotopic dependence shows that the motion response includes position information and that the motion-onset VEPs are not generated solely in the higher extrastriate areas (MT or MST).

Keywords: Motion-onset; VEP; Visual field

1. Introduction

According to literature data there are three visual channels transferring the visual information from the retina to the striatum. One of them, the parvocellular (sustained) system, is the form and colour oriented channel, the second, magnocellular (transient) one, carries predominantly motion information (Livingstone & Hubel, 1988). The third pathway, koniocellular, was not so thoroughly examined yet and its contribution to visual processing is only partially understood so far (Hendry & Calkins, 1998). The channels are named in accordance with the relay LGN cells belonging to. After entrance of these channels to visual cortex (the primary visual area V1—Brodmann's area 17), they become more mutually interconnected. The magnocellular channel continues to V2, V3A and MT (V5) extrastriate areas as the ''magnocellular pathway'' or ''parietal (dorsal) stream'' mainly responsible for processing of motion and space information. The parvocellular pathway coming in V2 (temporal–ventral stream) is involved in perception of colours and shapes (Tootell, Hadjikhani, Mendola, Marrett, & Dale, 1998; Ungerleider & Desimone, 1986).

Because of separate deficit of these pathways in some neuro-ophthalmic disorders like open angle glaucoma, multiple sclerosis, optic neuritis, amblyopia, etc. (e.g. Arakawa, Tobimatsu, Kato, & Kira, 1999; Klistorner & Graham, 1999; Kubová & Kuba, 1992; Kubová, Kuba, Juran, & Blakemore, 1996), it is quite important to develop examination technique for an objective selective assessment of the visual pathways function.

* Corresponding author. Tel: +420 49 581 6332; fax: +420 49 551 3597.
E-mail address: jan.kremlacek@lfhk.cuni.cz (J. Kremláček).

0042-6989/$ - see front matter © 2004 Elsevier Ltd. All rights reserved.
doi:10.1016/j.visres.2004.07.002

Our research group has been working for years on methods comprising motion oriented visual evoked potentials (VEPs) and magnocellular (dorsal) pathway examination (Kuba & Kubová, 1992). It is not easy to obtain an independent magnocellular system VEPs response, more likely it is possible to recognise it within VEPs as a specific component. Our previous results have shown that a negative component timed at about 160 ms (N1) in the motion-onset visual evoked potentials (M-VEPs) displays very high contrast sensitivity (Kubová, Kuba, Spekreijse, & Blakemore, 1995) as it was formerly described in single unit examination of magnocellular pathway in monkeys (Kaplan & Shapley, 1986).

The magnocellular input is formed from Y ganglion cells of retina whose receptive fields are mainly distributed in extrafoveal (even very peripheral) parts of retina. Therefore, the N1 peak of the M-VEPs has much lower amplitude decay than the pattern-reversal VEPs (Meredith & Celesia, 1982) in peripheral visual stimulation as proved by Muller, Gopfert, Schlykowa, and Anke (1990), Gopfert, Muller, and Simon (1990), and Schlykowa, van Dijk, and Ehrenstein (1993). They examined the M-VEPs for stimuli up to 23° of eccentricity and they were oriented solely to amplitude assessment.

Recent motion stimulation conditions enabled us to examine wider range of the visual field (VF) and therefore we tested properties of the motion-onset VEP peak latencies and amplitudes behaviour up to about 42° of eccentricity, while separate VF parts were stimulated. The presented study tried to verify possibilities of the motion-VEPs examination for objective perimetry.

2. Methods

2.1. Subjects

A group of 10 healthy adult subjects participated in this study (5 men; aged 22–41 years, 5 women; aged 25–49 years). They had neither ophthalmologic nor neurological abnormalities. All subjects had right dominant eye (determined by hole-in-card method). A written informed consent was obtained from every subject before the examination procedure.

2.2. Stimuli

The stimuli were generated on the 21 in. computer monitor ViewSonic with $42° \times 30°$ at 0.5 m viewing distance and 67 frames per second. The entire stimulated field of $84° \times 56°$ was achieved by consecutive changing of the fixation point to corners of the screen. Each stimulus field representing one quadrant of the VF was divided into five zones. The first one subtended central 7°, the next four zones were annular fields within boundaries at 7°, 16°, 28° and 42° of eccentricity. The last zone was limited by the size of the monitor screen to 42° horizontally and 28° vertically. For the stimulus appearance see Fig. 1. The sizes of all zones increased to the periphery according to the cortical magnification factor described by Rovamo and Virsu (1979) (see Fig. 2). Stimuli were playable animation files (Kremláček, Kuba, Kubová, & Vít, 1999).

Every zone was filled with a high contrast (96% by Michelson) checkerboard of a decreasing spatial frequency (0.5, 0.25, 0.166, 0.125 and 0.1 cycles/deg) and an increasing motion velocity (10, 20, 30, 40 and 50 deg/s) from the centre toward the periphery. The spatial frequencies and velocities were chosen to keep the temporal frequency equal to five cycles per second. The pattern in each zone moved in one of four cardinal directions in a pseudorandom order and also the

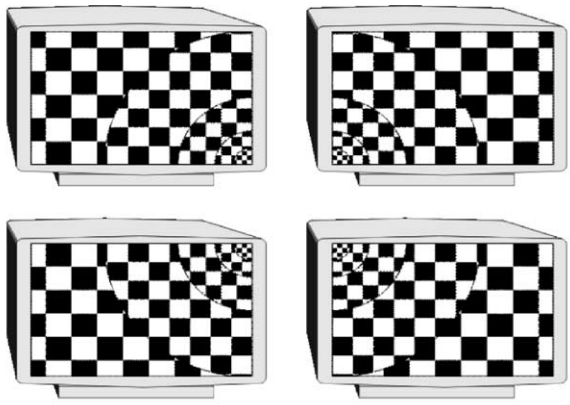

Fig. 1. Stimulus. The symbolic representation of the stimulus and the parameters of single zones.

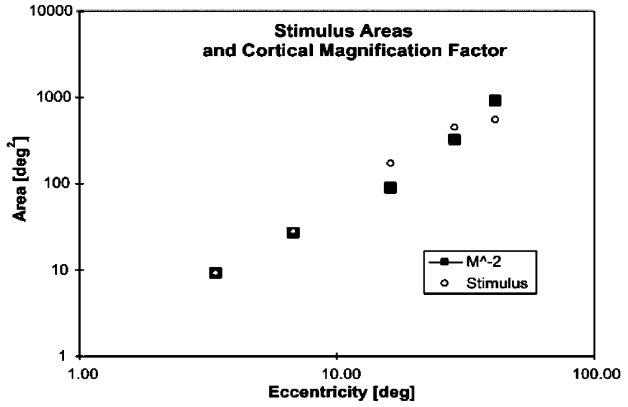

Fig. 2. Stimulated area and magnification factor. Relation of the stimulated area to the cortical magnification factor ($M = s/(1 + 0.33 * \text{ecc} + 0.00007 * \text{ecc}^3)$, where "ecc" represents eccentricity and "s" was a scaling coefficient 3.724).

sequence of successively stimulated zones was arranged not to stimulate any adjacent areas consecutively. Stimulus timing, constant for all zones, was 1 s of stationary pattern and 200 ms of motion. Mean stimulus luminance was of 17 cd/m^2.

2.3. Recordings

The acquisition was performed in darkened, sound attenuated, electromagnetically shielded room with the background luminance of 1 cd/m^2. During the experiment, the subjects sat in a comfortable dental chair with a neck support to reduce muscle artefacts and they were instructed to fixate an appropriate corner of the screen and not to follow the changes in stimulation field with their eyes. The correct fixation was monitored via infrared CCD camera located in the acquisition room. Every eye was examined separately in four quadrants with 100 stimuli, so that 20 single M-VEPs to each stimulus location was recorded. Unipolar registration was used from C_Z, O_Z and lateral temporo-occipital places 5 cm to the right (O_R) and 5 cm to the left (O_L) from O_Z. Right earlobe (A2) served as reference. The minimum set of recordings was chosen on the basis of previous topographical study concerning scalp distribution of the motion-onset VEPs (Kremláček & Kuba, 1999). The ground electrode was connected to the reference one. All electrodes impedances were kept below 5 kΩ. After amplification in the frequency band 0.3–100 Hz (Contact Precision Instruments—PSYLAB, System 5), signal was sampled at 500 Hz and off-line selectively averaged on a personal computer. The VEPs recording was synchronised with backward trace of the monitor electron beam, just before the first video frame of motion.

2.4. Analysis

M-VEPs latencies and amplitudes of P1, N1 and P2 peaks were determined in each derivation. The amplitudes were determined as P1–N1 (A1) and N1–P2 (A2) peak-to-peak differences.

The problem of systematic increase of latencies arose, when the upper part of VF was stimulated due to a delay between the synchronisation to the start of video-frame and the stimulation zone drawing (in the lower part of the screen). A correcting factor has been introduced to avoid time differences along vertical axis (related to the frame refresh ratio—order of milliseconds), while differences along horizontal axis were negligible (tens of microseconds—related to horizontal refresh ratio).

The bias was measured by a photocell in the centre of each stimulated segment. For refresh ratio of 67 Hz we have got correcting factor −12, −11, −8, −3 and −1 ms for segments 3.5°, 7°, 16°, 28° and 42° (respectively) in the upper half of the VF. Analogously when the lower half of the VF was stimulated we got −1, −3, −8, −11 and −12 ms for the segments 3.5°, 7°, 16°, 28° and 42° (respectively). The artificial delay was corrected before analysis.

To assure homogeneity of variance, we converted the absolute values of amplitudes into relative ones (because of higher interindividual variability; mean value of subject = 1) and logarithmically transformed latencies before statistical parameters were calculated.

Relative amplitudes and logarithmically transformed latencies were statistically analysed by analysis of variance of repeated measures (general linear model) with four within-subjects factors: stimulated eye, stimulated quadrant, eccentricity and the recording derivation. In case of statistical significance, multiple Fisher LSD post-hoc comparisons were used (Statistica v 5.5, USA). The alpha level of 0.05 was used for all statistical tests.

3. Results

The M-VEPs grand averages from all 10 subjects are presented in Fig. 3. The P1–N1–P2 peaks are well recognisable in all locations. According to ANOVA results, there are significant differences in the tested parameters among the stimulated quadrants and among the stimulus eccentricities (here with exception of the P1 latency). The parameters N1 and A1 and A2 showed also significant differences for recording derivations. The results are listed in details in Table 1 together with significant two- and three- way interactions. Post-hoc significant pairs for significant factors are also displayed. Since the left and right eyes did not differ significantly neither in the latencies nor in the amplitudes of the M-VEPs, subsequent quantitative comparisons were done for all twenty eyes together. Amplitude and latency comparisons among quadrants of the stimulated VF, eccentricities and recording derivations are shown in Figs. 4 and 5. Original values are represented in the figures, however statistical tests were done with transformed data (see Section 2 for details).

Since numerical description of all specified groups in these figures would be too extensive, there are only summarised values grouped for the stimulated quadrant in Table 2, eccentricity in Table 3 and recording derivation in Table 4. Particular values will be presented for discussed cases in the following description of post-hoc tests for significant ANOVA factors.

3.1. M-VEPs differences in visual field quadrants

The most significant factor affecting parameters of the motion-onset VEPs was the stimulated quadrant (see Tables 1, 2 and Fig. 3). The most prominent difference was between responses to the lower and upper part of the VF stimulation. There were significantly shorter

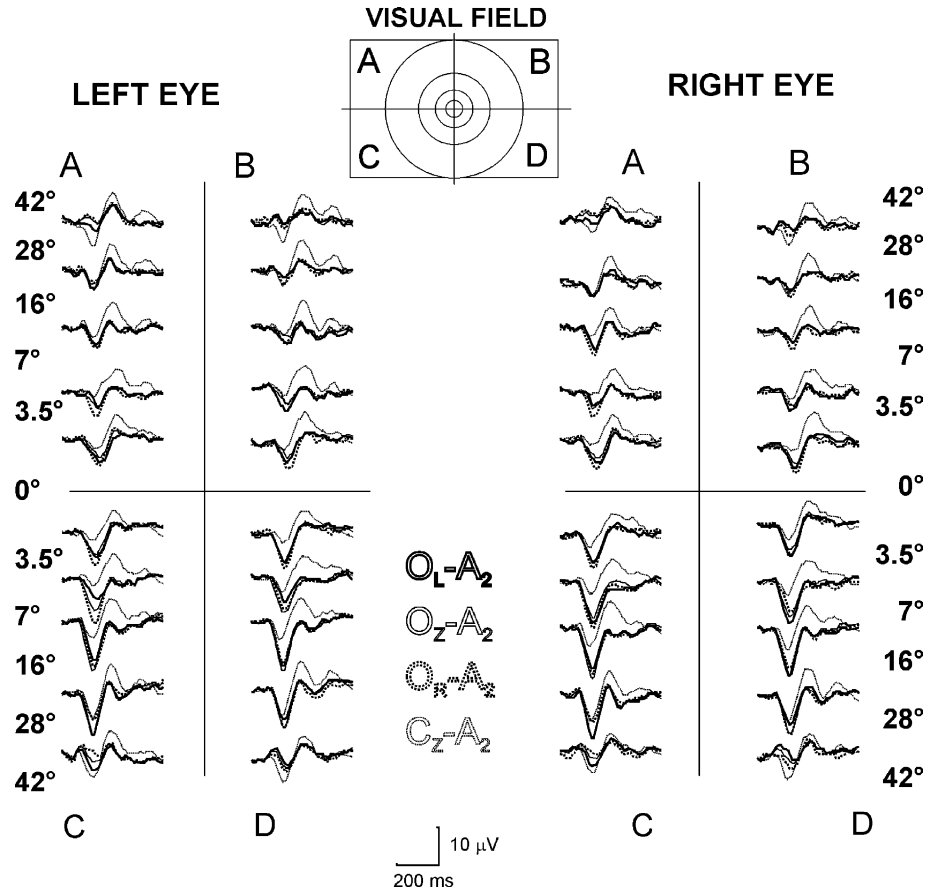

Fig. 3. Grand average motion evoked potentials over all 10 subjects. Responses from the left eye stimulation are presented on the left side and the right eye M-VEPs are on the right side. The solid bold and thin curves represent the left and the right occipital lead respectively; the dotted bold and thin ones are from the middle occipital and central derivation. The responses for the given stimulus eccentricities are divided into four quadrants of the VF.

latencies of P1 as well as N1 and larger amplitudes of A1 and A2 peaks in responses to lower quadrants stimulation. The P2 latencies were significantly shorter only for the left lower quadrant. An amplitude reversal (opposite polarity of main peaks in the upper hemifield stimulation—common in the pattern-reversal VEPs) was observed only in 10 (out of 400) responses (in three subjects for the lower hemifield stimulus at eccentricity 24–42°).

Comparison of responses to the left and right quadrants exhibited significant difference only in P1 latency for upper quadrants and in P2 latency for the lower quadrants. In summary, the left hemifield exhibited higher amplitudes and shorter VEP latencies and in the right upper (RU) quadrant stimulation the smallest amplitudes and the longest VEP latencies were recorded.

3.2. Role of eccentricity of stimulus area onto M-VEPs parameters

While the P1 latency was mostly dependent on the stimulated quadrant, eccentricity influenced mainly the N1 peak latency (see Table 1). For all stimulated eccentricities except the most peripheral one, we observed shortening of latencies. The amplitude dependence was not so straightforward. The highest amplitudes were recorded to stimulation of the fovea (0–3.5°) and eccentricity 7–24°. There was a distinct drop of amplitudes in parafoveal stimulation (3.5–7°). For more details concerning the influence of stimulus eccentricity see Table 3, Figs. 4 and 5. Results of the post-hoc tests are listed in Table 1.

3.3. Influence of recording place for M-VEPs parameters

The derivation strongly influenced the N1 peak latency and both evaluated amplitudes. In the post-hoc comparison significant difference between all occipital and the central recording site was found. The N1 latency recorded in C_Z was significantly shorter and amplitude of A2 higher than in the occipital derivations. In contrary, the amplitude A1 had smaller amplitudes in C_Z compared to the rest of derivations. For detailed description see Figs. 4, 5 and Tables 1, 4.

Table 1
Results of significance tests in repeated measure ANOVA in five parameters (rows) for four within-subject factors

	Quadrant {1}	Eccentricity {2}	Eye {3}	Derivation {4}	Interaction			
					1 * 2	2 * 3	2 * 4	1 * 2 * 4
P1[a]	$F(3,27) = 32.2$ $p < 0.001$ [LU LD] [RU RD] [LU RU] [LU RD] [LD RU]	$F(4,36) = 2.06$ $p = 0.16$	$F(1,9) = 0.01$ $p = 0.93$	$F(3,27) = 1.74$ $p = 0.18$	$F(12,108) = 5.12$ $p < 0.001$	$F(4,36) = 3.31$ $p < 0.05$	$F(12,108) = 3.79$ $p < 0.001$	$F(36,324) = 3.09$ $p < 0.001$
					1 * 2	1 * 4	1 * 2 * 4	2 * 3 * 4
N1	$F(3,27) = 16.61$ $p < 0.001$ [LU LD] [RU RD] [LU RD] [LD RU]	$F(4,36) = 8.32$ $p < 0.001$ [1 2] [1 3] [1 4] [1 5] [2 3] [2 4] [4 5]	$F(1,9) = 0.60$ $p = 0.46$	$F(3,27) = 19.62$ $p < 0.001$ [O_L O_Z] [O_L C_Z] [O_R C_Z] [O_Z C_Z]	$F(12,108) = 4.54$ $p < 0.001$	$F(9,81) = 2.08$ $p < 0.05$	$F(36,324) = 2.74$ $p < 0.001$	$F(12,108) = 1.96$ $p < 0.05$
					1 * 2	1 * 2 * 4		
P2	$F(3,27) = 2.99$ $p < 0.05$ [LU LD] [LD RD] [LD RU]	$F(4,36) = 10.38$ $p < 0.001$ [1 2] [1 3] [1 4] [1 5] [2 3] [2 4] [4 5]	$F(1,9) = 0.82$ $p = 0.39$	$F(3,27) = 0.64$ $p < 0.61$	$F(12,108) = 4.03$ $p < 0.001$	$F(36,324) = 1.48$ $p < 0.05$		
					1 * 2	1 * 4	2 * 4	1 * 2 * 4
A1	$F(3,27) = 38.18$ $p < 0.001$ [LU LD] [RU RD] [LU RD] [LD RU]	$F(4,36) = 23.40$ $p < 0.001$ [1 3] [1 5] [2 3] [2 5] [3 5] [4 5]	$F(1,9) = 0.11$ $p = 0.75$	$F(3,27) = 4.90$ $p < 0.01$ [O_L C_Z] [O_R C_Z] [O_Z C_Z]	$F(12,108) = 5.61$ $p < 0.001$	$F(9,81) = 2.32$ $p < 0.05$	$F(12,108) = 15.05$ $p < 0.001$	$F(36,324) = 4.08$ $p < 0.001$
					1 * 2	1 * 4	2 * 4	1 * 2 * 4
A2[b]	$F(3,27) = 29.69$ $p < 0.001$ [LU LD] [RU RD] [LU RD] [LD RU]	$F(4,36) = 12.20$ $p < 0.001$ [1 2] [1 5] [2 3] [2 4] [3 5] [4 5]	$F(1,9) = 1.76$ $p = 0.22$	$F(3,27) = 10.41$ $p < 0.001$ [O_L C_Z] [O_R C_Z] [O_Z C_Z]	$F(12,108) = 4.13$ $p < 0.001$	$F(9,81) = 2.25$ $p < 0.05$	$F(12,108) = 14.03$ $p < 0.001$	$F(36,324) = 4.31$ $p < 0.001$

The significantly ($p < 0.05$) different pairs of parameters by post-hoc tests are listed in square brackets. For eccentricity: the numbers 1–5 represent the eccentricities of 0–3.5°, 3.5–7°, 7–16°, 16–24° and 24–42°. The interactions are listed only for significant values $p < 0.05$. Each interaction cell includes information about the factor combination; significant pairs by post-hoc test are not listed because of large number of combinations.

[a] P1 additional significant interaction $1 * 2 * 3 * 4$ $F(36,324) = 1.57$; $p < 0.05$.

[b] A2 two additional significant interactions $2 * 3 * 4$ $F(12,108) = 2.08$; $p < 0.05$ and $1 * 2 * 3 * 4$ $F(36,324) = 1.83$; $p < 0.01$.

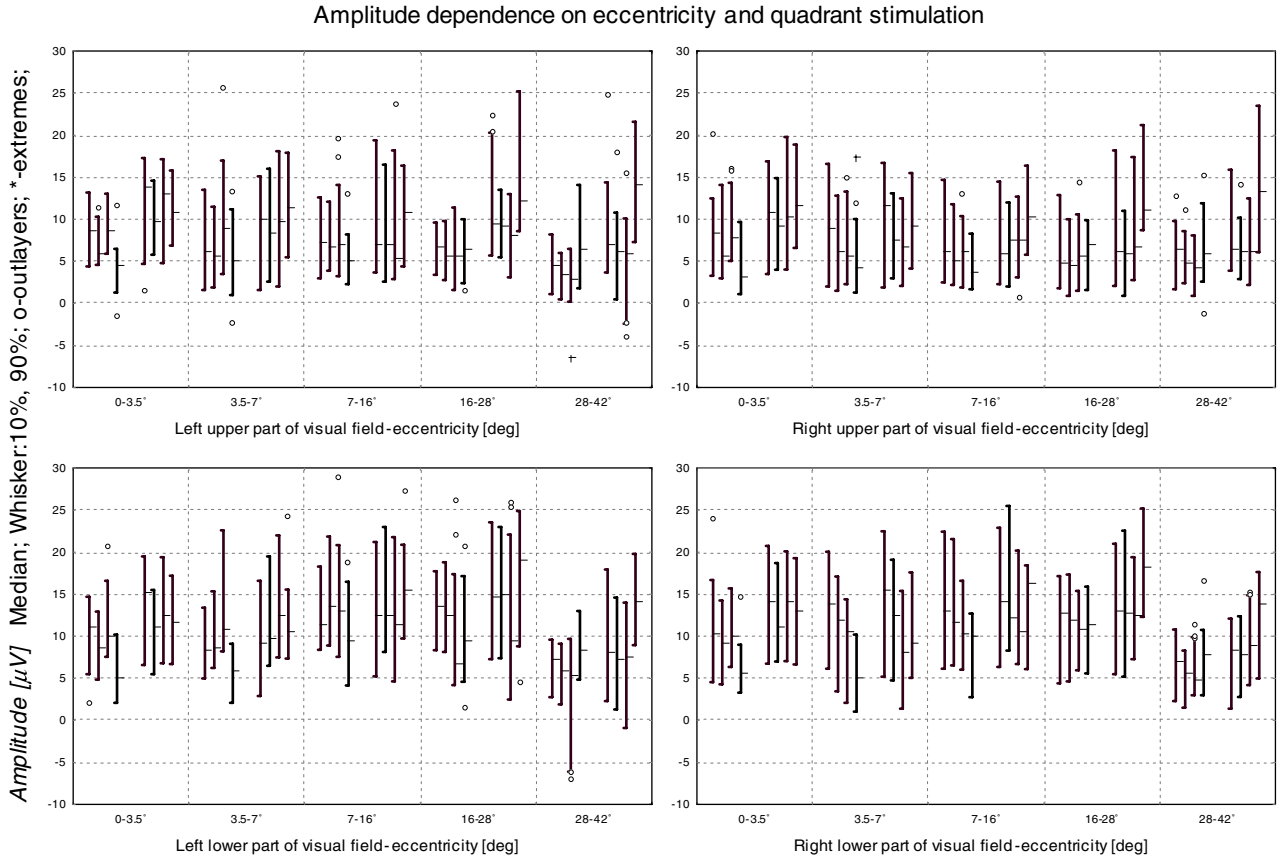

Fig. 4. Summarised amplitude plot. Median and 10–90 percentile range of the observed amplitudes for eccentricities 0–3.5°, 3.5–7°, 7–16°, 16–24°, 24–42° from all recorded derivations are plotted in four graphs corresponding to the stimulated quadrant of the visual field. The order of the plots from left to right in each eccentricity: A1 from O_L, O_Z, O_R and C_Z derivations and A2 from O_L, O_ZO, $_R$ and C_Z derivations. Each range plot represents 20 values (two eyes of 10 subjects). The outlayers (value > 75th (<25th) percentile + 1.5 * (75th–25th percentile)) are marked as open circles and extremes (value > 75th (<25th) percentile + 3 * (75th–25th percentile)) as star symbol. The figure shows smaller amplitudes to stimulation in the upper part of VF ($p < 0.001$), reduced responses to the most peripheral stimulus ($p < 0.001$) and increasing amplitude with eccentricity in C_Z.

4. Interactions between influencing factors

In the previous comparison, the factors congregate responses that are not of the same basis by nature (i.e. for the derivation factor the responses to the left and right part of the VF are grouped and, therefore, other significant differences between lateral derivations hided). However, an interaction of factors like the second order interaction of derivation and stimulated quadrant should address the problem. Because the interactions are increasing the number of comparisons (eccentricity and quadrant yield 180 comparisons) and higher interactions than of the second order are difficult to interpret, the following description will be restricted to the most interesting results. All relations described below are listed in Table 1 and in Figs. 4 and 5.

4.1. Eccentricity vs. quadrant

The interaction between stimulated quadrant and eccentricity was significant for all tested parameters. The observed shortening of latencies with increasing eccentricity of stimulation (except the most peripheral stimulation) was stronger for lower quadrants (mainly the left one). The P1 peak displayed even increasing latency with eccentricity for the upper right quadrant stimulation. Accordingly, the lower stimulated quadrants displayed higher amplitudes in eccentricities 7–28°, while the upper quadrants did not. The shortest latencies and the lowest response variability were observed for the left lower quadrant in eccentricity from 16° to 28°.

4.2. Eccentricity vs. derivation

This interaction was significant for both A1 and A2 amplitudes and for P1 latency. In the occipital derivations, there was tendency to decrease amplitudes toward the periphery. The response to the most peripheral stimulus exhibited significantly smaller amplitudes compared to the rest of the VF. However, the responses recorded from the C_Z derivation displayed increasing amplitudes and shortening of the P1 latency toward periphery of the VF. The P1 latency in C_Z derivation was significantly

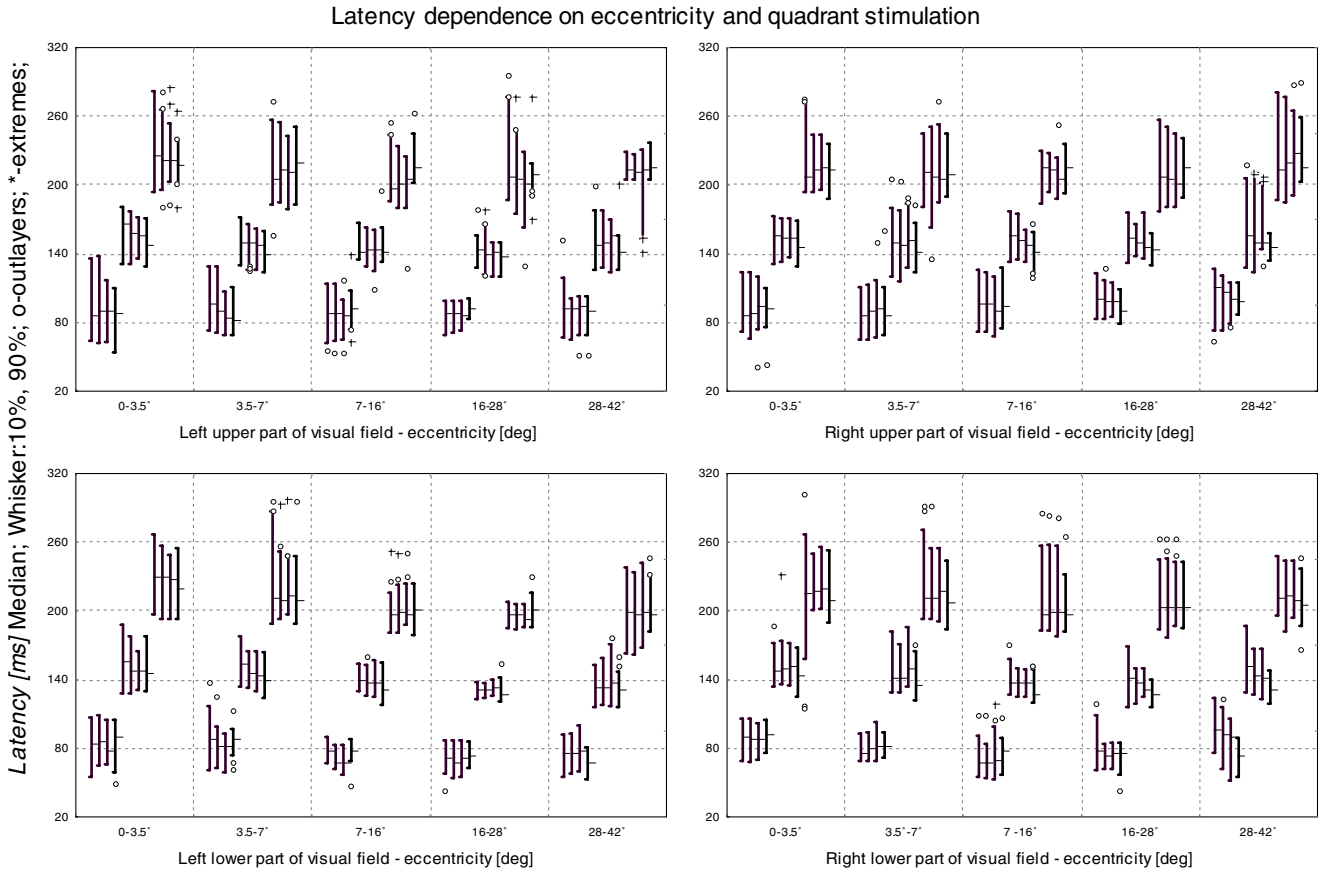

Fig. 5. Summarised latency plot. Latency distribution of the three latency parameters—P1, N1 and P2 across the visual field recorded from four derivations O_L, O_Z, O_R and C_Z. The figure arrangement as well as the statistical representation is similar as in Fig. 4. In each eccentricity there is a triplet (P1, N1 and P2 latencies) of four (O_L, O_Z, O_R and C_Z) range plots. Each range plot covers 20 absolute corrected latencies (two eyes subjects). The plots from the lower part of the visual field display shorter latencies especially for eccentricities over 7° ($p < 0.001$). The shortest latencies and the least variability are manifested in the left lower quadrant for eccentricities of 16–28°. Note the change in trend of occipital parameters (the first three in each quaternary range plots) that is strong mainly in N1 latency. The eccentricity of the 7–16° is a breaking point from which the signal propagation differs from that in the central visual field.

Table 2
Descriptive statistics of examined parameters grouped by the quadrants (cumulate the four recording derivations and all eccentricities)

Quadrant	LU (left upper) Median (25–75%) [*]; *N*[–]	RU (right upper) Median (25–75%) [*]; *N*[–]	LD (left lower) Median (25–75%) [*]; *N*[–]	RD (right lower) Median (25–75%) [*]; *N*[–]
A1 [*μV]	5.9 (4.0–8.7); 359	5.7 (3.4–8.4); 369	9.3 (6.9–12.5); 392	9.2 (5.7–13.0); 393
A2 [*μV]	9.2 (5.8–13.2); 357	8.6 (5.0–12.1); 369	11.7 (8.1–16.4); 392	11.9 (7.9–16.4); 393
P1 [*ms]	89 (77–98); 350	96 (84–108); 365	76 (67–87); 392	79 (70–90); 389
N1 [*ms]	145 (136–156); 350	148 (138–158); 363	136 (129–150); 392	139 (130–149); 390
P2 [*ms]	211 (201–224); 351	213 (199–226); 361	202 (193–219); 392	208 (196–228); 390

Each cell contains the median with lower and upper quartile and number of observations.

Table 3
Descriptive statistics of examined parameters grouped by the eccentricity (cumulate the four recording derivations and all quadrants)

Eccentricity	0–3.5° Median (25–75%) [*]; *N*[–]	3.5–7° Median (25–75%) [*]; *N*[–]	7–16° Median (25–75%) [*]; *N*[–]	16–28° Median (25–75%) [*]; *N*[–]	28–42° Median (25–75%) [*]; *N*[–]
A1 [*μV]	8.0 (5.4–10.6); 307	7.3 (4.7–11.5); 310	9.0 (5.5–12.4); 303	8.3 (5.5–12.4); 303	5.6 (3.5–8.0); 290
A2 [*μV]	11.7 (8.3–15.0); 306	9.4 (5.8–13.0); 309	10.6 (6.6–15.8); 303	11.1 (7.2–17.4); 303	8.3 (5.2–12.3); 290
P1 [*ms]	88 (77–101); 308	83 (75–95); 303	80 (68–92); 303	81 (71–93); 300	87 (74–100); 282
N1 [*ms]	150 (139–162); 307	145 (135–159); 302	138 (132–150); 303	135 (129–145); 301	143 (130–153); 282
P2 [*ms]	219 (204–235); 306	211 (199–229); 301	202 (192–220); 303	201 (193–211); 302	210 (198–225); 282

Each cell contains the median with lower and upper quartile and number of observations.

Table 4
Descriptive statistics of examined parameters grouped by recording derivation (cumulate the four recording quadrants and all eccentricities)

Derivation	O_L Median (25–75%) [*]; *N*[–]	O_Z Median (25–75%) [*]; *N*[–]	O_R Median (25–75%) [*]; *N*[–]	C_Z Median (25–75%) [*]; *N*[–]
A1 [*μV]	8.7 (5.4–12.2); 374	7.4 (4.7–11.1); 377	7.9 (5.1–10.9); 385	6.3 (3.9–9.2); 377
A2 [*μV]	10.0 (6–14.7); 374	9.4 (5.9–12.9); 377	9.1 (5.8–13.8); 385	12.5 (9.1–16.4); 375
P1 [*ms]	85 (73–99); 370	83 (71–97); 372	84 (72.5–96.5); 380	85 (75–95); 374
N1 [*ms]	145 (133–159); 370	143 (133–154); 372	144 (134–154); 381	137 (127–147); 372
P2 [*ms]	207 (197–227); 369	207 (196–225); 370	209 (195–224); 380	209 (198–223); 375

Each cell contains the median with lower and upper quartile and number of observations.

shorter compared to occipital ones in the most peripheral eccentricity.

4.3. Eccentricity vs. quadrant vs. derivation

There were no significant differences between the responses to the left vs. right visual hemifield across all eccentricities. However, there was distinct dependence of the N1 parameters on the eccentricity (see Figs. 5 and 6). Therefore, we tested correlations of the amplitude and latency differences between the lateral leads and eccentricity. Among all parameters tested, the most significant ($p < 0.001$) Pearson correlation coefficients were found between the N1 latency difference and eccentricity: −0.406 (+0.295) for the left (right) hemifield stimulated. The dependence of latency difference on eccentricity expressed by linear regression of medians (“least squares estimate”) for left hemifield has form of $dN1_{LHF} = 6.453 - 0.266 * \text{eccentricity}$, where $dN1_{LHF}$ is the difference of the main negative peak latency between the left and right occipital lead. Related right hemifield dependence is $dN1_{RHF} = -2.262 + 0.256 *$ eccentricity (see Fig. 7). In amplitudes significant ($p < 0.001$) correlations $r = 0.335$ ($r = 0.363$) between A1 (A2) and eccentricity were found only for left hemifield activation. The best fit of medians has form $dA1_{LHF} = -2.628 - 0.96 * \text{eccentricity}$ ($dA2_{LHF} = -2.848 - 1.16 * \text{eccentricity}$), where $dA1_{LHF}$ is difference between the left and right occipital lead in A1 (A2) amplitude. The graph in Fig. 6 displays the $dA1_{LHF}$

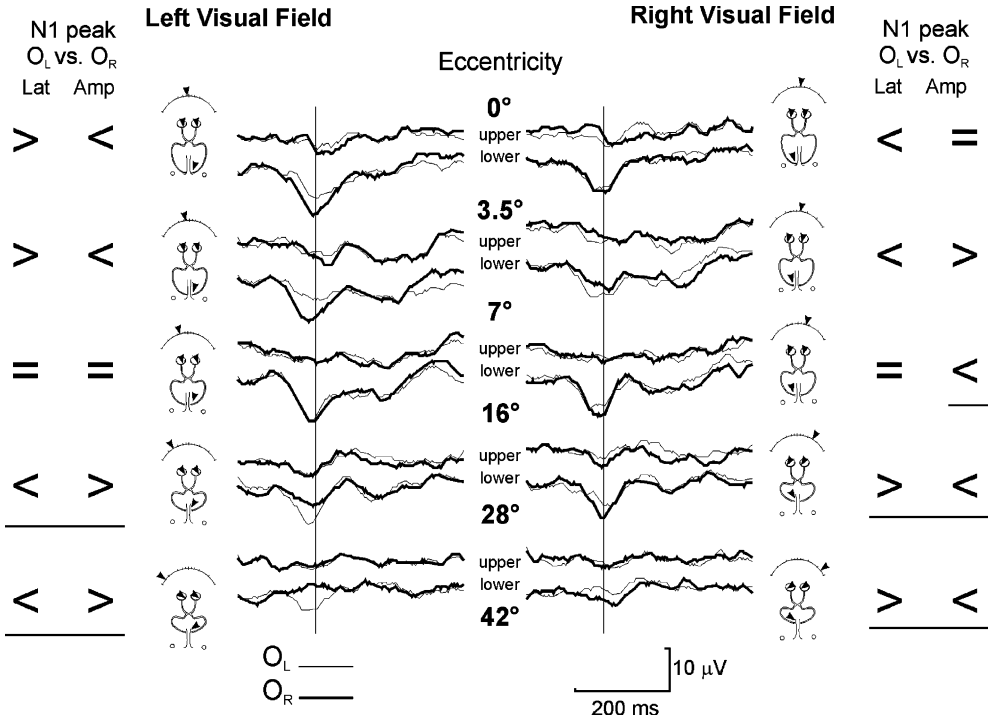

Fig. 6. Single subject response laterality. The single subject M-VEPs recorded from the left and right occipital derivation to left vs. right upper and lower quadrants of the stimulus field in different eccentricities. The responses from left occipital site (O_L) plotted as a thin line, the right one (O_R) as a bold line are superposed for common stimulus location. The left column shows responses to both left quadrants, while in the right column there are responses to the respective parts of the right hemifield. Sideways to the M-VEPs, there is a symbolic projection from visual field to the corresponding part of the primary visual cortex and a comparison of latency and amplitude for O_L and O_R for the particular eccentricity. The underlined symbols do not correspond to the predicted activation.

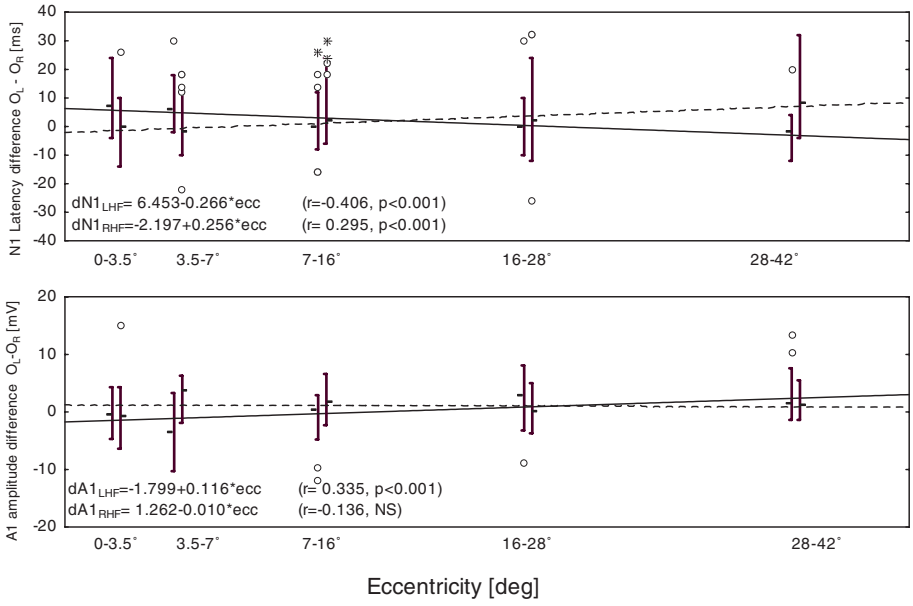

Fig. 7. Relation of hemifield stimulation and M-VEPs latency and amplitude. The comparisons of differences between the dominant negative peak of motion-onset VEPs from the left and right occipital derivation for the left (the first range plot with left median sign) and right (the second range plot with right sign of median) part of the stimulated field. The upper graph shows latency (N1 peak) and the lower one amplitude (A1) difference relation to the eccentricity. Each range plot (median, 10 and 90 percentile) covers 40 values (10 subjects, 2 eyes and 2 quadrants—upper and lower). The medians of differences were approximated by best linear fit (solid line for left part of visual field and dotted for the right one). The equation together with correlation and significance describing each fit and data are listed in appropriate graph. The most interesting information is that the latency differences for both hemifields are crossing at 16.6°, which does not correspond to the classical visual information propagation (see Section 5).

dependence on the eccentricity. In one subject, the paradoxical lateralization was not present at all.

5. Discussion and conclusions

It is remarkable that in our experiments the readable M-VEPs were recorded in all 20 areas covering central $56° \times 84°$ of visual field. A significant amplitude decrease was not observed up to 28° of eccentricity (in the central 56° of the VF). The observed reduction of the response in the most peripheral stimulation, despite of the highest velocity (50 deg/s) and the spatial frequency of 0.1 cycle/deg, can be explained by smaller than optimal size of the stimulated area in this eccentricity. The last zone was constrained to 60% (by limited size of the stimulating monitor) of the ideal field respecting the cortical magnification factor, which can be important (Schlykowa et al., 1993). Since there is limited ability of the system to detect the used motion in the far periphery (our most peripheral stimulated zone), we can consider this as another reason for the amplitude drop (Anderson, Drasdo, & Thompson, 1995).

We observed that the behaviour of latency parameters (P1, N1, P2) correlate well with receptive field properties. Reduction of the retinotopic correspondence with latency was demonstrated for example by the amount of significant differences among quadrants (P1-5 differences, N1-4 and P2-3). That corresponds well to the hypothesis of visual signal processing from simple–physical parameters to more complex–perceptual representation. The variability increased with latency (see Fig. 5). The amplitude parameters A1 and A2 exhibited similar behaviour (see Fig. 5), since both of them are related to the dominant negative peak N1.

The finding that the lower half of VF displays larger amplitudes can be explained by the recording positions. The electrodes above the inion, in the O_Z level, emphasise lower VF responses, which is caused by different orientation of generators, as reported for the pattern reversal VEPs P100 peak (e.g. by Lehman & Skrandies, 1979; Orban & Muller, 1991; Yu & Brown, 1997). Another explanation is a superiority of upper hemiretina in our visual system, which was reported not only for electrophysiological parameters (Skrandies & Baier, 1986) and for psychophysical parameters but also anatomical evidence exists (for example Rubin, Nakayama, & Shapley, 1996). The first specified reason for the recorded M-VEPs differences in the upper and lower hemifields is clearly plausible but it can explain amplitude changes only, however, the shorter latencies from the lower part of the VF seem to be likely a result of different information processing from the horizontal hemifields. Therefore, we suggest that motion-onset VEPs are influenced by both mechanisms.

Differences between the lower and upper hemifields are in accordance with the cited works using by pattern-reversal stimulation. However, the possibility that

motion onset activates the same generators is not likely, because the N1 shows high contrast sensitivity (Kubová et al., 1995) and the pattern-reversal VEPs are measurable only within 12° of the central VF (Meredith & Celesia, 1982). Moreover, our motion-onset data did not display the main peak polarity shift, presented in the pattern-reversal stimuli (e.g. Lehman, Meles, & Mir, 1977). This fact makes the motion evoked potentials more suitable for VF examination and a promising candidate for retrochiasmatic lesions detection because of smaller variability, which is the cause of hemifield testing rejection by the International Federation for Clinical Neurophysiology (Celesia et al., 1993).

Lateralization of the maximal VEPs amplitude was reported in motion onset processing (e.g. Hollants-Gilhuijs, DeMunck, Kubová, van Royen, & Spekreijse, 2000; Kubová, Kuba, Hubáček, & Vít, 1990). Despite of this fact, we did not selectively averaged the dominant responses to get difference in dominant vs. non-dominant hemispheres. Anyhow, there was slight (9%) enhancement of responses present under left occipito-temporal derivation in our group (see Table 4).

However, the lateralization of the N1 peak was strongly dependent on the vertical hemifield and on the eccentricity of stimulation. When the central part up to 17° of eccentricity was stimulated, shorter latencies were measured over the contralateral hemisphere to the stimulated hemifield. When the eccentricity of the stimulus was more than 17°, then the N1 response had shorter latency over the ipsilateral hemisphere = paradoxical lateralization. The shorter latencies were accompanied by larger amplitude in the interval from 3.5° to 28° of eccentricity. The most central and the most peripheral regions exhibited equal amplitudes but not latencies (see Fig. 7).

Since the stimulus comprises not only motion-onset information but also information about the place where the motion occurred, the simplest explanation of that phenomenon would be that there is a differentially positioned generator of the N1 peak with respect to the stimulus eccentricity in the visual field. For eccentricity over 17° the generator is in such position that the major projection onto the scalp is not under the closest electrode, but under the contralateral one. The effect was described for pattern reversal stimulation of vertical hemifields as the ''paradoxical lateralization'' (Barrett, Blumhardt, Halliday, Halliday, & Kriss, 1976). However, this hypothesis does not explain the latency dependence on eccentricity, which should not be influenced by projection onto the scalp.

From above mentioned findings an argument arises that the motion-onset VEP (especially P1 and N1 peaks generators) are, at least partially, retinotopically dependent and organised (the quadrant and eccentricity are the most influencing M-VEPs factors). Moreover, there is latency shortening and amplitude increase of the N1 peak toward periphery in the C_Z derivation. The N1 responses under C_Z location were about 8 ms shorter in average than in the occipital region. The most probable explanation is that none of these peaks fully corresponds to the low level detection of motion which occurs much earlier at about 71–75 ms in the MT or MST areas (Buchner et al., 1997; ffytche, Guy, & Zeki, 1995). But there are also other structures (V2, V3A), likely involved in the peak formation, which are retinotopical. The N1 peak then would be a composition of many different sources along the dorsal stream from the primary visual cortex to the frontal eye fields. Similar finding was already reported for multielectrode VEP recording to full field motion-onset stimulus in our previous papers (Kremláček & Kuba, 1999; Kremláček, Kuba, & Kubová, 1998). The N1 peak was composed of two independent components: the earlier with maximum at 120 ms in frontal region and later one at 160 ms in temporo-occipital areas. From the latency inconsistency between occipital and central recordings it is likely that the dominant N1 wave is not generated in the feedforward processing but rather during a backward run, which was shown to be important part of the visual processing (Pascual-Leone & Walsh, 2001). The further evidence for this statement arises from single cells recording in macaque, when all direct visual areas (V1, V2, V3, V4, MT, MST and FEF) were activated in feedforward run before 100 ms (for review see Lamme & Roelfsema, 2000, or Bullier, 2001).

It is necessary to point out the interindividual variability of latencies that was surprisingly reduced for the left lower quadrant at eccentricity of 7–28° (see Fig. 4). Since there is a lateralization of the motion processing as discussed above we can speculate that at the particular location the visual processing generators and motion detectors are so close in cortex that their mutual contribution to the resulting VEP was compact. The place of the minimum variability can be closely related to the reported lateralization of motion processing. To confirm fully the specified hypothesis, it is necessary to make a source analysis of a multielectrode recording and possibly event related fMRI examination (since sustained activity is not corresponding to the transient EP). However, the facilities of methods with less numerous channel recordings have not been fully utilised yet.

The finding that we can record a response up to eccentricity of 42° suggests that such stimulus configuration can be used in neuro-ophthalmologic electrophysiology as an objective VF examination. This is very important for the practical applications, since nowadays there are multifocal VEP approaches to solve question of objective perimetry but they are usually restricted to excentrities up to 25° (Jedynak & Skrandies, 1998; Klistorner, Graham, Grigg, & Billson, 1998) mostly by stimulus parameters. For example method based on the pattern-onset EPs could bring useful results only up to

about 15° of eccentricity (Hoffmann, Straube, & Bach, 2003).

The multifocal techniques employ a rapid stimulus presentation and therefore they activate different cortical areas compared to the motion-onset N1 peak which have a strong adaptation effect (Bach & Ullrich, 1994). Therefore, our technique is complementary to mentioned multifocal perimetry and can be used to reduce false positive findings. Further, the used parameters focused to the magnocellular system function could give reasonable additional diagnostic information (Kubová & Kuba, 1992).

Acknowledgments

This work was supported by the Grant agency of the Czech Republic (grant No. 309/02/1134) and by the Czech Ministry of Education (CEZ: J13/98: 111100008).

References

Anderson, S. J., Drasdo, N., & Thompson, C. M. (1995). Parvocellular neurons limit motion acuity in human peripheral vision. *Proceedings of the Royal Society of London. Series B: Biological Sciences, 22*, 129–138.

Arakawa, K., Tobimatsu, S., Kato, M., & Kira, J. (1999). Parvocellular and magnocellular visual processing in spinocerebellar degeneration and Parkinson's disease: an event-related potential study. *Clinical Neurophysiology, 110*, 1048–1057.

Bach, M., & Ullrich, D. (1994). Motion adaptation governs the shape of motion-evoked cortical potentials. *Vision Research, 34*, 1541–1547.

Barrett, G., Blumhardt, L., Halliday, A. M., Halliday, E., & Kriss, A. (1976). A paradox in lateralization of the visual evoked response. *Nature, 261*, 253–255.

Buchner, H., Gobbele, R., Wagner, M., Fuchs, M., Waberski, T. D., & Beckmann, R. (1997). Fast visual evoked potential input into human area V5. *Neuroreport, 8*, 2419–2422.

Bullier, J. (2001). Integrated model of visual processing. *Brain Research Reviews, 36*, 96–107.

Celesia, G., Bodis-Wollner, I., Chatrian, G., Harding, G., Sokol, S., & Spekreijse, H. (1993). Recomended standards for electroretinograms and visual evoked potentials. Report of IFCN committee. *Electroencephalography and Clinical Neurophysiology, 87*, 421–436.

ffytche, D. H., Guy, C. N., & Zeki, S. (1995). The parallel visual motion inputs into areas V1 and V5 of human cerebral cortex. *Brain, 118*, 1375–1394.

Gopfert, E., Muller, R., & Simon, E. M. (1990). The human motion onset VEP as a function of stimulation area for foveal and peripheral vision. *Documenta Ophthalmologica, 75*, 165–173.

Hendry, S. H., & Calkins, D. J. (1998). Neuronal chemistry and functional organization in the primate visual system. *Trends in Neurosciences, 21*, 344–349.

Hoffmann, M. B., Straube, S., & Bach, M. (2003). Pattern-onset stimulation boosts central multifocal VEP responses. *Journal of Vision, 3*, 432–439.

Hollants-Gilhuijs, M. A. M., DeMunck, J. C., Kubová, Z., van Royen, E., & Spekreijse, H. (2000). The development of hemispheric asymmetry in human motion VEPs. *Vision Research, 40*, 1–11.

Jedynak, A., & Skrandies, W. (1998). Functional perimetry combined with topographical VEP analysis. *International Journal of Neuroscience, 93*, 117–132.

Kaplan, E., & Shapley, R. M. (1986). The primate retina contains two types of ganglion cells, with high and low contrast sensitivity. *Proceedings of the National Academy of Sciences of the United States of America, 83*, 2755–2777.

Klistorner, A. I., & Graham, S. L. (1999). Early magnocellular loss in glaucoma demonstrated using the pseudorandomly stimulated flash visual evoked potential. *Journal of Glaucoma, 8*, 140–148.

Klistorner, A. I., Graham, S. L., Grigg, J. R., & Billson, F. A. (1998). Multifocal topographic visual evoked potential: improving objective detection of local visual field defects. *Investigative Ophthalmology Visual Science, 39*, 937–950.

Kremláček, J., & Kuba, M. (1999). Global brain dynamics of transient visual evoked potentials. *Physiological Research, 48*, 303–308.

Kremláček, J., Kuba, M., & Kubová, Z. (1998). Electrophysiological manifestation of first-order motion perception. *Perception, 27*(Suppl.), 192–193 (Abstract).

Kremláček, J., Kuba, M., Kubová, Z., & Vít, F. (1999). Simple and powerful visual stimulus generator. *Computer Methods and Programs in Biomedicine, 58*, 175–180.

Kubová, Z., & Kuba, M. (1992). Clinical application of motion-onset visual evoked potentials. *Documenta Ophthalmolmologica, 81*, 209–218.

Kubová, Z., Kuba, M., Hubáček, J., & Vít, F. (1990). Properties of visual evoked potentials to onset of movement on a television screen. *Documenta Ophthalmologica, 75*, 67–72.

Kubová, Z., Kuba, M., Juran, J., & Blakemore, C. (1996). Is the motion system relatively spared in amblyopia? Evidence from cortical evoked responses. *Vision Research, 36*, 181–190.

Kubová, Z., Kuba, M., Spekreijse, H., & Blakemore, C. (1995). Contrast dependence of motion-onset and pattern-reversal evoked potentials. *Vision Research, 35*, 197–205.

Kuba, M., & Kubová, Z. (1992). Visual evoked potentials specific for motion onset. *Documenta Ophthalmolmologica, 80*, 83–89.

Lamme, V., & Roelfsema, P. (2000). The distinct modes of vision offered by feedforward and recurrent processing. *Trends in Neurosciences, 23*, 571–579.

Lehman, D., Meles, H., & Mir, Z. (1977). Average multichannel EEG potential field evoked from upper and lower hemiretina: latency differences. *Electroencephalography and Clinical Neurophysiology, 43*, 725–731.

Lehman, D., & Skrandies, W. (1979). Multichannel evoked potential fields show different properties of human upper and lower hemiretina systems. *Experimental Brain Research, 35*, 151–159.

Livingstone, M., & Hubel, D. (1988). Segregation of form, color, movement, and depth: anatomy, physiology, and perception. *Science, 240*, 740–749.

Meredith, J. T., & Celesia, G. G. (1982). Pattern-reversal visual evoked potentials and retinal eccentricity. *Electroencephalography and Clinical Neurophysiology, 53*, 243–253.

Muller, R., Gopfert, E., Schlykowa, L., & Anke, D. (1990). The human motion VEP as a function of size and eccentricity of the stimulation field. *Documenta Ophthalmologica, 76*, 81–89.

Orban, D., & Muller, W. (1991). Amplitudes of visually evoked cortical responses due to full-field stimulation and to stimulation with four half-fields. *Documenta Ophthalmologica, 202*, 100–104.

Pascual-Leone, A., & Walsh, V. (2001). Fast backpropagation from the motion to the primary visual area necessary for visual awareness. *Science, 292*, 510–512.

Rovamo, J., & Virsu, V. (1979). An estimation and application of the human cortical magnification factor. *Experimental Brain Research, 37*, 459–510.

Rubin, N., Nakayama, K., & Shapley, R. (1996). Enhanced perception of illusory contours in the lower versus upper visual hemifields. *Science, 271*, 651–653.

Schlykowa, L., van Dijk, B. W., & Ehrenstein, W. H. (1993). Motion-onset visual-evoked potentials as a function of retinal eccentricity in man. *Brain Research: Cognitive Brain Research, 1*, 169–174.

Skrandies, W., & Baier, M. (1986). The standing potential of the human eye reflects differences between upper and lower retinal areas. *Vision Research, 26*, 577–581.

Tootell, R. B., Hadjikhani, N. K., Mendola, A. D., Marrett, S., & Dale, A. M. (1998). From retinotopy to recognition: fMRI in human visual cortex. *Trends in Cognitive Sciences, 2*, 174–183.

Ungerleider, L. G., & Desimone, R. (1986). Cortical connections of visual area MT in the macaque. *The Journal of Comparative Neurology, 248*, 190–222.

Yu, M. Z., & Brown, B. (1997). Variation of topographic visually evoked potentials across the visual field. *Ophthalmic Physiological Optics: The Journal of the British College of Ophthalmic Opticians (Optometrists), 17*, 25–31.